

P.001/004
the advent of computers and electronic calculators, the computational use of diagrams has declined, but they still are used widely for depicting atmospheric structure, visualizing processes, and determining stability.

A Smattering of History

The origins of atmospheric thermodynamic diagrams in their present form can be traced back to the late 1800s. Around this time progress in understanding the thermodynamics of atmospheric processes and unraveling the mysteries of cloud formation was accompanied by a greater need for estimates of temperature changes in saturated ascent. The task at hand was, in essence, solving Eq. (6.130). A quantitative saturated adiabatic theory originated with the work of William Thomson (Lord Kelvin), described in a paper read in 1862 (not published until 1865). But the distinction between saturated and unsaturated ascent was made some 20 years before Thomson's work. James Espy, an American meteorologist, used experimental data to estimate both moist and dry adiabatic lapse rates. He constructed and used a device he called a *nepheloscope* (an expansion cloud chamber) to make these estimates. His pioneering contributions to atmospheric thermodynamics can be found in his 1841 treatise *Philosophy of Storms*. Espy is best known for his disagreement with William Redfield about the way winds are distributed in storms. James McDonald, in the second of two excellent historical papers, argues that this controversy may have obscured Espy's important contributions to atmospheric thermodynamics.

Although Thomson established the theoretical basis for describing saturated adiabatic processes, McDonald avers that Joule may have provided the conceptual impetus for Thomson's work. McDonald also notes that Thomson's paper is difficult to follow because it is poorly written and because volumes rather than masses are used to formulate the problem. A year before publication of this paper, a Swiss meteorologist, Reye, submitted a paper that elegantly treated saturation theory, including a formulation of and exact solution to the differential equation describing the moist adiabatic process. Reye used his results to determine the stability of a saturated layer and compared it with that of a dry layer. McDonald argues that Reye gave the definitive theory with little room for improvement and that his work was independent of Thomson's.

Despite these early treatments, an 1874 paper by an Austrian meteorologist, Hann, often is cited as the origin of saturation theory even though his purpose was to summarize previous work of Thomson and Reye and an 1868 paper by a French engineer, Deslin. Hann also gave a table of temperatures and pressures for saturated adiabatic ascent.

In 1884 Heinrich Hertz, a physicist best known for his experimental verification of the electromagnetic theory of light and immortalized by the unit of frequency, the Hertz (Hz), developed a thermodynamic diagram that eliminated the need for tedious calculations of thermodynamic variables. The overall features of this diagram do not differ substantially from those used today.

Although it is not clear why Hertz became interested in the saturated adiabatic process, this may have been a consequence of the interest of his mentor, Helmholtz, in hydrodynamics. McDonald unearthed one reference suggesting that Hertz's work on thermodynamic diagrams was a recreational activity. Hertz included on his dia-

gram moist adiabats calculated as pseudoadiabats, although he did not refer to them as such.

In 1888 von Bezold, a Bavarian meteorologist, carefully derived a mathematical description of the pseudoadiabatic process. In addition to calculating temperature differences between this process and the adiabatic process, he considered a complete cloud cycle involving pseudoadiabatic ascent followed by dry adiabatic descent. By this process condensational warming (enthalpy of vaporization transformed into a temperature increase) followed by the removal of water through precipitation can result in net warming of the atmosphere. Although global net evaporation of water from the surface is balanced by precipitation over long times, pseudoadiabatic processes yielding precipitation result in warming of the atmosphere, which helps balance net radiative cooling. The work of von Bezold provided the framework for describing atmospheric energetics associated with precipitation.

Although several thermodynamic diagrams were developed following the pioneering work of Hertz, only two are in common use today: the skew T -log p (often referred to briefly as skew T) and the tephigram. We discuss the details of construction for only the skew- T diagram; the general approach can be applied to any diagram. Isopleths included on standard thermodynamic diagrams are pressure (isobars), temperature (isotherms), potential temperature (dry adiabats), equivalent potential temperature or wet-bulb potential temperature (moist adiabats), and saturation mixing ratio. Although computers and pocket calculators have diminished the need for diagrams to calculate thermodynamic variables, these tools now make it easier to construct diagrams and display atmospheric data on them.

Skew T -log p Diagram

The basic coordinates of the skew T -log p diagram (also known as the skew emagram) are temperature T and $-\ln p$ (see Fig. 6.5). Isotherms are rotated 45° relative to isobars to increase the angle between isotherms and adiabats, thereby facilitating the analysis of stability. Because of the nearly exponential variation of pressure with height, $-\ln p$ is approximately proportional to height. Many skew- T diagrams include a height scale based on the U.S. Standard Atmosphere, which is convenient for estimating heights for data obtained as a function of pressure.

Dry adiabats are curves defined by

$$T = \Theta \left(\frac{p}{p_o} \right)^{R_d/c_{pd}} \quad (6.145)$$

for constant Θ . Because the difference between T and Θ is small compared with either of them, we can rewrite this equation so that the (approximate) shape of dry adiabats is evident:

$$-\ln \left(\frac{p}{p_o} \right) \approx \frac{c_{pd}}{R_d} \left(1 - \frac{T}{\Theta} \right) \quad (6.146)$$

For constant Θ , the curve of $-\ln(p/p_o)$ versus T is approximately a straight line with negative slope (see Fig. 6.6). The 45° skew of isotherms results in adiabats about 90° to isotherms.

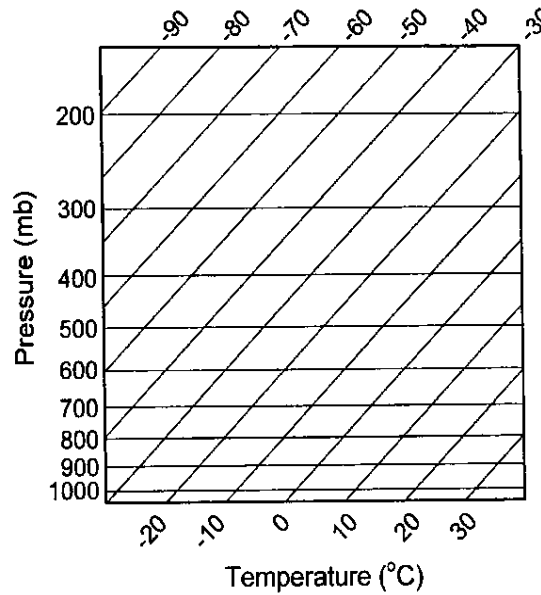


Figure 6.5 Basic coordinates of the skew-*T* diagram.

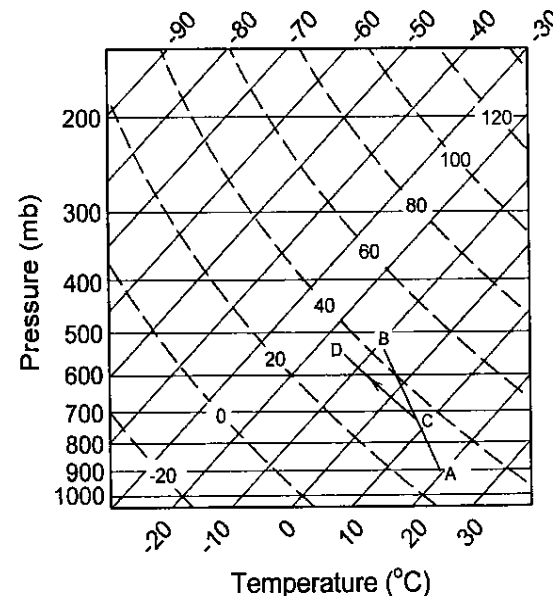


Figure 6.6 Skew-*T* diagram of Fig. 6.5 with dry adiabats (dashed) added. The line segment AB shows the temperature structure for a hypothetical sounding between about 500 and 900 mb. Dry adiabatic ascent from 725 mb is illustrated by the line segment CD.

Even with only dry adiabats on a thermodynamic diagram, we can illustrate its use. To estimate potential temperature, for example, plot temperature and pressure; the corresponding potential temperature is obtained directly from the dry adiabat. If a sounding is used to display atmospheric temperature as a function of pressure, stability at each height is evident from the slope of the sounding compared with that of the dry adiabat it intersects.

We must carefully distinguish between lines on a diagram that display atmospheric structure and those that depict processes. Figure 6.6 shows temperature versus pressure in a layer AB, the lapse rate for which is less than dry adiabatic. Air in this layer is therefore stable. This application illustrates atmospheric structure. A process can be illustrated by imagining air to be taken from some pressure within the layer to another pressure; the temperature variation (provided there is no condensation) follows a dry adiabat on the diagram. Figure 6.6 shows adiabatic ascent of air originating at C and terminating at D; the temperature of a parcel along this adiabat can be read directly from the diagram.

Moist adiabats (adiabats for processes undergone by air at saturation) can be included on a thermodynamic diagram by numerically integrating Eq. (6.130) for a pseudoadiabatic process ($c_p = c_{pd} + w_s c_w$). These adiabats often are labeled with Θ_w values because the temperature at 1000 mb is the wet-bulb potential temperature. Moist adiabats as they appear on a skew-*T* diagram are illustrated in Fig. 6.7. At low pressures and temperatures moist adiabats become parallel to dry adiabats. Each moist adiabat could be labeled with a Θ_e value corresponding to the dry adiabat the moist adiabat converges to at low pressure.

From the definition of mixing ratio at saturation ($w = w_s$), it follows that

$$p = e_s(T) + \frac{\epsilon e_s(T)}{w_s} \quad (6.147)$$

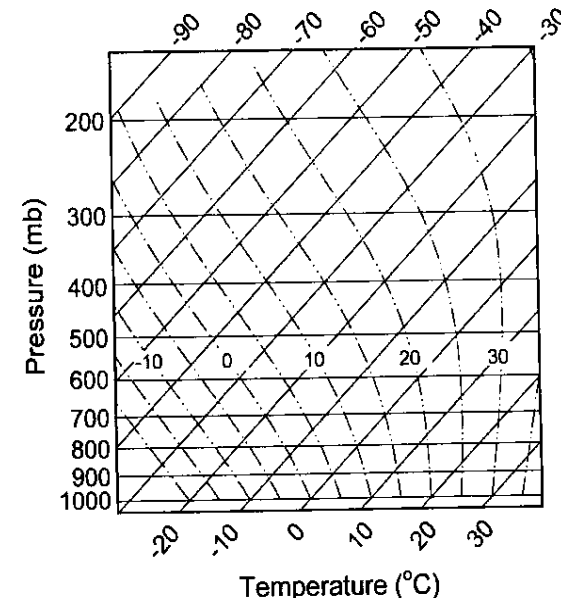


Figure 6.7 Skew-*T* diagram of Fig. 6.5 with moist adiabats (chain-dashed) added; the isopleths are labeled with the value of the wet-bulb potential temperature (temperature at 1000 mb).

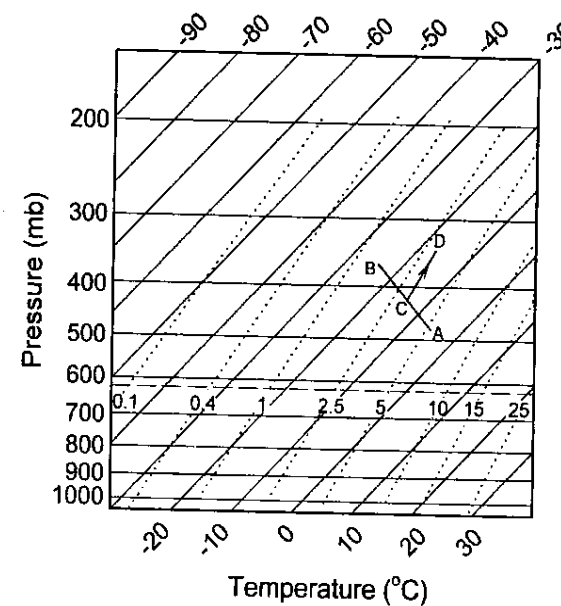


Figure 6.8 Skew-*T* diagram of Fig. 6.5 with constant mixing ratio (g/kg) isopleths (dotted) added. The horizontal dashed line is at 622 mb. At this level the saturation mixing ratio (expressed in g/kg) is approximately numerically equal to the saturation vapor pressure (expressed in mb).

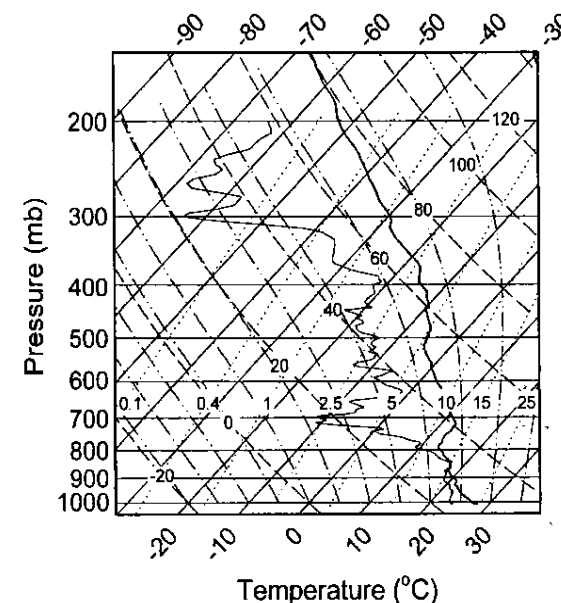


Figure 6.9 A complete skew-*T* diagram obtained by combining Figs. 6.6–6.8. The thick solid line shows a sounding of temperature; the thin solid line is the corresponding dew point.

For constant w_s , Eq. (6.147) defines a p - T curve, which can be depicted on a skew-*T* diagram. Lines of constant saturation mixing ratio, which are approximately straight, are shown in Fig. 6.8. The dew point of unsaturated air at any pressure p determines the mixing ratio w because $w = w_s(T_d, p)$. The moisture structure of a sounding can be illustrated by plotting dew point or w as a function of pressure. In unsaturated ascent or descent of a parcel w is conserved. The dew point variation in such a process can be determined from the skew-*T* diagram by following the constant-mixing-ratio line and finding the temperature at each pressure. This is shown in Fig. 6.8 for a layer with mixing ratio profile AB . If air at the middle of this layer (C) is displaced adiabatically to a lower pressure, the variation in dew point can be determined along CD because w is constant (in the absence of condensation).

Mixing ratio is approximately $\epsilon e/p$, where $\epsilon = 0.622$. To express w in g/kg instead of kg/kg, we have to multiply by 1000:

$$w \approx 622 \frac{e}{p} \quad (6.148)$$

Thus at $p = 622$ mb, the value of w (in g/kg) is numerically equal to e (in mb), which provides a quick way to estimate saturation vapor pressure from a skew-*T* diagram. For example, in Fig. 6.8 follow the 0°C isotherm until it intersects the 622 mb isobar. By interpolation, the corresponding (saturation) mixing ratio is about 6 g/kg, and thus the saturation vapor pressure at 0°C is about 6 mb (6.11 mb is the correct value).

A skew-*T* diagram with all isopleths previously described is shown in Fig. 6.9. To provide more resolution, actual diagrams have isopleths at more frequent intervals. Consequently, these diagrams may appear more cluttered than that in Fig. 6.9.

With both moist and dry adiabats on the same diagram, the asymptotic approach

of a moist to a dry adiabat at low pressure is evident. To illustrate how atmospheric temperature and moisture structure can be depicted on a skew-*T* diagram, we show a sounding of temperature and dew point as a function of pressure obtained from a ship in the central equatorial Pacific. Two variables are required to specify the thermodynamic state of unsaturated air at a given pressure. For saturated air only one variable is required (liquid water is not represented on a skew-*T* diagram). A detailed stability analysis of the sounding shown in Fig. 6.9 is deferred to the following section, but for the moment we note the stable inversion layer at 850 mb. Above this inversion the mixing ratio drops markedly.

Relations among many of the thermodynamic variables discussed in this and previous chapters can be illustrated on thermodynamic diagrams, in particular, a skew-*T* diagram (Fig. 6.10). Isotherms and most isobars have been removed for clarity.

Consider air with pressure p , temperature T , and dew point T_d , which uniquely determine the mixing ratio and potential temperature. If a parcel characterized by these two thermodynamic variables is lifted adiabatically, during ascent they follow the appropriate w and Θ isopleths. Temperature and dew point decrease until the two are equal at the lifting condensation level (LCL). From Eq. (6.13) and the definition of dew point it follows that $w = \text{constant}$ is a curve of dew point versus pressure. Thus the LCL is where the Θ and w isopleths extending from the original temperature and dew point intersect. As ascent continues past the LCL, temperature and mixing ratio follow a moist adiabat.

The equivalent potential temperature of a parcel can be estimated by following the moist adiabat to low pressure and obtaining the Θ value for the dry adiabat to which the moist adiabat converges. If this adiabat is not labeled with a value (on the diagram), follow it down to 1000 mb and estimate the temperature at this level (see Fig. 6.10). If, after ascent to high level, the parcel descends along the dry adiabat to the

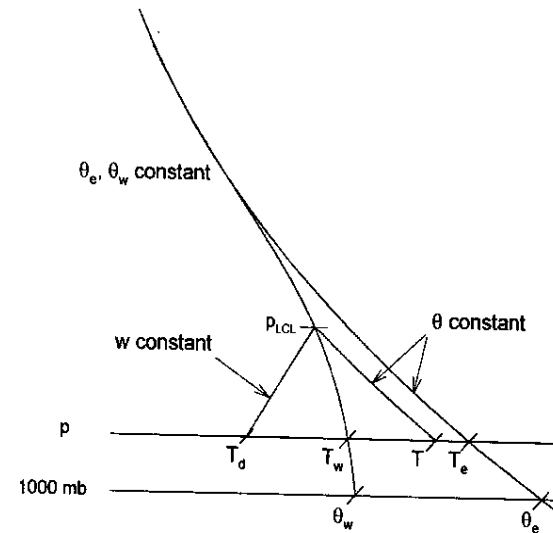


Figure 6.10 Depiction of thermodynamic variations on a skew- T diagram from which all but the essential isopleths are omitted.

original pressure rather than 1000 mb, the resulting temperature is the equivalent temperature T_e . This (adiabatic or, more correctly, pseudoadiabatic) equivalent temperature differs from the (isobaric) equivalent temperature discussed in Section 6.4. Unlike that equivalent temperature, the pseudoadiabatic equivalent temperature is defined by a real process. A parcel is lifted from some initial level dry adiabatically until it reaches saturation. Above this level temperature decreases at the moist adiabatic rate and any condensed water is removed. The parcel is lifted to low pressure until all its water vapor condenses and then is returned dry adiabatically to the original pressure. The final temperature is the (pseudoadiabatic) equivalent temperature. Although this process is not isobaric, the initial and final pressures are the same.

Wet-bulb temperature and wet-bulb potential temperature also can be estimated on a skew- T diagram (see Fig. 6.10). Imagine the parcel to be lifted dry adiabatically to the LCL, then taken moist adiabatically back to its original pressure. Water must be added to the parcel to maintain saturation. The temperature at this level is sometimes called the adiabatic wet-bulb temperature and differs from the (isobaric) wet-bulb temperature defined in Section 6.4. The term *adiabatic wet-bulb temperature* is confusing given that the process defining the (isobaric) wet-bulb temperature is also adiabatic. To add to the confusion, the process defining Θ_w is really pseudoadiabatic because water vapor is added to the parcel (it is not a closed system). If the moist adiabat is followed down to 1000 mb, the corresponding temperature is the wet-bulb potential temperature (see Fig. 6.10). Representing wet-bulb temperature on a skew- T diagram again illustrates that $T_d \leq T_w \leq T_e$.

The work done in a cyclic process represented by a closed curve on a skew- T diagram is proportional to the area enclosed by this curve. To show this, note that the work done in such a process can be written as [see Eq. (4.185)]

$$\oint p \, dv = \oint d(pv) - \oint v \, dp = - \oint v \, dp \quad (6.149)$$

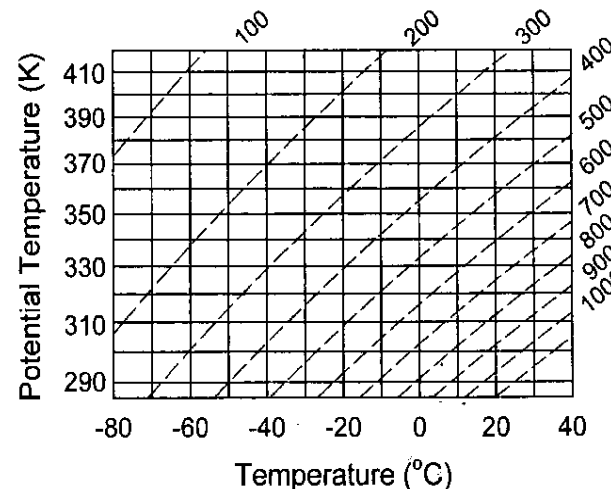


Figure 6.11 Basic coordinates of the tephigram. Isobars are dashed lines.

By using the ideal gas law Eq. (6.149) becomes

$$\oint p \, dv = - \oint \frac{RT}{p} \, dp = R \oint T (-d \ln p) \quad (6.150)$$

The skew- T diagram has coordinates T and $-\ln p$, and hence Eq. (6.150) shows that work done is proportional to the area enclosed on this diagram; the skew of the axes merely changes the proportionality factor.

Tephigram

The tephigram (also known as the T - s diagram) derives its name from the coordinates temperature T and entropy ($c_p \ln \Theta$), sometimes denoted by ϕ . The basic coordinates for this diagram are shown in Fig. 6.11; the abscissa is temperature, and the ordinate is $\ln \Theta$. Isobars are generated from the Poisson relation; moist adiabats and saturation mixing lines are calculated as for the skew- T diagram but transformed to T - $\ln \Theta$ coordinates. A complete diagram is shown in Fig. 6.12. If this diagram is rotated 45° clockwise, it appears similar to the skew- T diagram, but isobars are slightly curved and dry adiabats are straight lines.

The area on a tephigram enclosed by a closed curve is proportional to the work done in the cyclic process represented by the curve. To show this, use the definition of potential temperature

$$c_p \ln \Theta = c_p \ln T - R \ln p + \text{const} \quad (6.151)$$

in Eq. (6.148)

$$\oint p \, dv = R \oint T (-d \ln p) = c_p \oint T d \ln \Theta - c_p \oint dT = c_p \oint T d \ln \Theta \quad (6.152)$$